<u>This paper is submitted to the Special Session "Input-output Modelling and Supply Chain Resilience".</u>

Cobalt supply disruptions reshape China's decarbonization pathway

Yuanchen Sun[1,2], *Sanmang Wu*[1,2*], *Shantong Li*[3], *Jianwu He*[3]

1.School of Economics and Management, China University of Geoscience (Beijing), Beijing 100083, People's Republic of China;

2.MOE Social Science Laboratory of Mineral Resources Security Governance, China University of Geosciences (Beijing), Beijing 100083, People's Republic of China;

3.Development Research Center of the State Council, Beijing 100010, People's Republic of China

Abstract

Securing critical minerals has become a central constraint on the energy transition and on the delivery of Nationally Determined Contribution (NDC) targets. Cobalt is a particularly acute case for China: the metal accounts for a vanishingly small share of aggregate output, yet it sits inside the traction-battery supply chain that supports the rapid electrification of road transport. This study couples a Bayesian network-Monte Carlo (BN-MC) risk model with the dynamic recursive China computable general equilibrium model (DRCCGE) to quantify how cobalt supply-chain disruptions propagate through the macroeconomy, the energy system, and CO_2 emissions from 2023 to 2060. Three findings emerge. First, refined cobalt contributes less than 0.01% of China's GDP, but a disruption generates losses far larger than the sector's own size. Under an extreme 2027 disruption with DRE=80%, China's real GDP falls by 0.29% relative to the baseline, and the tail value at risk reaches US$61.4 billion. Second, aggregate CO_2 emissions change only modestly, but this muted total masks an unfavourable structural shift. Cobalt scarcity suppresses electric-vehicle deployment and raises transport CO_2 emissions, while the contraction of electricity-intensive manufacturing and coal power offsets much of that increase. Third, although the disruption imposes short-run economic losses, the long-run adjustment under a binding NDC constraint reallocates capital away from electric vehicles and batteries towards wind, solar, nuclear, and CCS, accelerating parts of the energy transition. The analysis identifies the

mechanism through which critical-mineral constraints reshape mitigation pathways and provides quantitative evidence for early-warning systems and policy responses to mineral supply-chain disruption.
Keywords: cobalt supply-chain disruption; NDC target; energy transition; computable general equilibrium model

1 Introduction

The Paris Agreement requires the world to hold the increase in global mean temperature to well below 2°C above pre-industrial levels and to pursue efforts to limit warming to 1.5°C, a goal that demands a profound transformation of national energy systems (IPCC, 2022). China is a major participant, contributor, and increasingly a shaper of global climate governance. It has committed to peak carbon emissions before 2030 and achieve carbon neutrality before 2060, and it has announced a 2035 Nationally Determined Contribution (NDC) target that would reduce economy-wide net greenhouse gas emissions by 7%-10% from their peak level. Large-scale deployment of new-energy vehicles (NEVs) is central to this mitigation pathway. Road transport accounts for about 10% of China's CO_2 emissions and remains one of the fastest-growing sources of emissions (IEA, 2024). Supported by industrial policy and market demand, China's NEV industry has expanded at exceptional speed: sales exceeded 15 million vehicles in 2025, annual penetration approached 50%, and China became the world's largest producer and consumer of NEVs (China Association of Automobile Manufacturers, 2025).

This rapid expansion depends on secure supplies of critical minerals, especially cobalt. Cobalt is an essential component of many lithium-ion battery cathode chemistries and therefore underpins the scaling of electric vehicles (EVs), portable electronics, and other low-carbon and high-technology applications (IEA, 2024; Olivetti et al., 2017). Under the International Energy Agency's net-zero emissions scenario, global cobalt demand is expected to rise sharply, roughly doubling from current levels by 2035 and tripling by 2040 (IEA, 2025). Supply, however, is geographically concentrated to an unusual degree. The Democratic Republic of the Congo (DRC) accounts for about 74% of global mine production (USGS, 2024), and roughly 90% of that material is refined in China. China holds more than 75% of global refined cobalt capacity (Cobalt Institute, 2024), yet its dependence on imported cobalt resources is as high as 98%. China therefore occupies a paradoxical position: it leads global EV manufacturing, but the upstream raw-material base remains externally constrained (Sun et al., 2019).

The geographical concentration of the cobalt supply chain, when combined with geopolitical instability, transport disruption, and export-control risk, makes cobalt a potential systemic bottleneck for the energy transition. In 2018, the DRC revised its Mining Code, designated cobalt as a "strategic mineral", and raised mining royalties from 2% to 10%; battery demand then helped push London Metal Exchange cobalt prices to a historic high of roughly US$95,000 per tonne. In 2020, the COVID-19 pandemic disrupted global supply chains and mine operations in the DRC, creating temporary cobalt shortages whose network effects amplified related economic losses by a factor of two to three (Guan et al., 2020). In 2024, the Red Sea shipping crisis reduced Suez Canal container throughput by 82%, impairing a critical maritime route linking African mining regions to downstream markets (UNCTAD, 2024). In February 2025, the DRC imposed a cobalt export ban; Glencore, the world's largest cobalt producer, invoked force majeure and suspended some cobalt deliveries. After the ban expired, the regime shifted to quota management, with 2026 export quotas around 34% below historical export volumes. These episodes can delay EV deployment, increase the oil dependence of road transport, and ultimately weaken China's ability to deliver its NDC and carbon-neutrality goals (Sun et al., 2019; Tang et al., 2021; Zeng et al., 2022).

Existing studies have examined critical-mineral constraints on the energy transition from several angles. At the strategic level, Sovacool et al. (2020) argue that low-carbon transitions require coordinated governance of mineral supply chains, while IEA (2021) projects that clean-energy technologies could increase mineral demand fourfold by 2040. In the battery-materials literature, Olivetti et al. (2017) identify cobalt and lithium as potential constraints on battery scale-up. Xu et al. (2020) estimate that global EV-battery demand for cobalt could rise 17- to 19-fold between 2020 and 2050, exceeding current supply capacity. Zeng et al. (2022), using dynamic material-flow analysis, further show that even low-cobalt battery technologies and recycling may not prevent cobalt shortages from constraining EV deployment during 2028-2033. Together, these studies show that cobalt faces a structural risk of supply-demand imbalance over the next one to three decades, driven by demand scale, limited substitution potential, and upstream supply bottlenecks.

The measurement of critical-mineral supply risk has also advanced substantially. One line of work constructs indicator systems to compare minerals by supply risk and strategic importance. Graedel et al. (2012) and Schrijvers et al. (2020) develop assessment frameworks that incorporate supply concentration, recycling, geopolitical exposure, and related dimensions, providing tools for identifying strategic minerals. Building on this tradition, Gulley et al. (2018) compare China and the United States in their competition for minerals required by emerging technologies;

Manberger and Johansson (2019) evaluate the geopolitical risks of metals used in renewable energy technologies; and Church and Crawford (2020) examine how rising mineral demand may spill over into conflict risks in resource-rich developing economies. A second line of work uses complex networks and Bayesian networks to characterize shock propagation and uncertainty. Klimek et al. (2015) trace cascading effects along upstream and downstream links in global trade networks. Garvey et al. (2015) develop a Bayesian-network framework for supply-network risk propagation. Shao et al. (2024) bring probabilistic inference into supply-chain modelling, making it possible to represent both parameter uncertainty and stochastic disruption events. These approaches motivate the supply-risk measurement strategy used here. Because the cobalt chain is highly connected and exposed to multiple risk sources, this study couples a Bayesian network with Monte Carlo simulation to estimate disruption risk exposure along China's cobalt supply chain. The framework captures linkages and shock transmission at the firm and node level, identifies heterogeneity that would be hidden by sectoral aggregation, and then embeds the resulting supply shock in a dynamic CGE model so that micro-level supply-chain risk can be linked to macroeconomic and energy-system adjustment.

The literature has therefore established cobalt's strategic value for the global energy transition and has documented substantial supply-chain risks. It has not yet answered how far those risks could impede the transition once they pass through the full economic system. Computable general equilibrium (CGE) models are well suited to this problem because they represent how exogenous sectoral shocks propagate through prices, input-output linkages, factor markets, and feedback effects across the economy. CGE analysis therefore provides a disciplined theoretical and quantitative framework for evaluating policy and supply shocks (Li and Zhai, 1997; Li et al., 2010). Recent studies have begun to integrate critical minerals into CGE frameworks, thereby bridging mineral-resource constraints and macroeconomic-energy modelling. Shi et al. (2025), using CGE and related models, show that critical-mineral supply-demand constraints can sharply limit China's renewable-energy capacity and directly slow the energy transition. Wei et al. (2025) evaluate full IPCC AR6 mitigation pathways in a CGE framework and reveal the systemic effects of critical-mineral scarcity on the feasibility of global energy-transition pathways. Yet most existing studies focus on aggregate mineral supply-demand balances and transition-path feasibility. They rarely represent the uncertainty of cobalt-specific supply-chain disruption, and they do not trace how a cobalt shock travels from the upstream mineral chain to batteries, EV deployment, transport decarbonisation, and the wider general equilibrium.

This gap matters because the relevant policy question is not only whether enough cobalt exists in aggregate, but how a probabilistic disruption in a concentrated supply chain changes mitigation outcomes through the economy. Existing work provides a methodological basis for analysing the macroeconomic and energy consequences of mineral-market changes, but it does not integrate probabilistic supply-risk quantification with dynamic, multi-sector CGE modelling. Without such integration, the full transmission chain from mineral disruption to battery manufacturing and transport emissions cannot be observed, and early-warning systems for cobalt risk remain incomplete. To address this gap, this study couples a BN-MC model with a CGE model to quantify the macroeconomic, energy-structure, and carbon-emissions effects of cobalt supply-chain disruption under China's energy transition. The contribution is threefold. First, the study links a probabilistic Bayesian network-Monte Carlo supply-risk model to a 42-sector recursive dynamic CGE model, establishing an explicit mapping from probabilistic critical-mineral disruption exposure to macroeconomic losses. Second, the method is designed for cobalt's unusual profile: cobalt represents only about 0.7% of the value of a traction battery, but it remains physically difficult to replace at scale. The model therefore adds a downstream productivity-transmission channel, beyond standard price transmission, to capture non-price effects such as production-line stoppages, yield losses, and coordination failure in supply chains. This design can be extended to other critical minerals that have low value shares but high physical indispensability. Third, the policy analysis traces the whole chain from cobalt ore to refined cobalt, traction batteries, EVs, and transport decarbonisation. It shows that sectoral emissions can move in opposite directions and cancel out in aggregate data, implying that climate-policy assessment must look below economy-wide totals to detect structural risk.

The rest of the manuscript is organised as follows. Section 2 describes the coupled BN-MC supply-chain risk model and DRCCGE framework, with particular attention to the fixed-factor cobalt-ore supply function and the embedding of disruption risk exposure. Section 3 explains the construction of the social accounting matrix, the separation of the refined cobalt sector, and the calibration of key parameters. Section 4 defines the baseline, NDC target, and cobalt disruption scenarios and describes the exogenous shock paths used in the simulations. Section 5 reports the transmission effects of cobalt supply-chain disruption on GDP, CO_2 emissions, and the energy structure. Section 6 summarises the main conclusions and develops policy implications.

2 Methods

The analytical core of this study is China's multi-sector DRCCGE model. The model is grounded in general equilibrium theory and describes the behaviour of producers, consumers, government, and external accounts through supply, demand, and market-clearing relationships. It contains production, factor, enterprise, household, government, and foreign-account modules, and the relationships among these modules are shown in Figure 1. The DRCCGE model has several defining features. On the production side, it uses nested constant-elasticity-of-substitution (CES) functions and a putty-clay capital specification that distinguishes between new and existing capital vintages. Labour is divided into agricultural, unskilled, and skilled labour, while households are divided into urban and rural groups. Imports follow the Armington assumption (Armington, 1969), exports follow a constant-elasticity-of-transformation (CET) specification, and the model is solved recursively over time. DRCCGE has developed into a policy-oriented CGE platform that can support Chinese policy analysis across economic development, trade, fiscal and tax policy, energy and environment, population, and sudden-disaster assessment (Li and He, 2009).

To represent the disruption risk facing China's refined cobalt supply under global supply-chain shocks, this study couples the BN-MC model with DRCCGE. The BN-MC model quantifies the cumulative distribution of China's cobalt supply-chain disruption risk exposure, and this distribution is then embedded in DRCCGE to trace the economic and energy-system consequences of cobalt supply constraints.

China's cobalt supply chain is mapped as a Bayesian network model $G = (V, E, P)$. The node set is$V = O \cup A$ and contains 76 supply nodes: 34 upstream mine nodes, 37 midstream enterprise nodes, and 5 Chinese refined cobalt enterprise nodes. The set $O = \{O_1, O_2, \ldots, O_n\}$ denotes the supply nodes, while the terminal aggregation node A represents China's total refined cobalt supply. The directed edge set is $E = E_1 \cup E_2$, where E_1describes the relationships through which risk factors affect nodes, and E_2describes upstream-downstream supply relationships. Pdenotes the collection of prior and conditional probabilities. The cobalt supply-chain BN model includes six risk factors for each of the 34 mine nodes, denoted $Risk_{M1}$-$Risk_{M6}$, and six risk factors for each of the 42 enterprise nodes, denoted $Risk_{C1}$-$Risk_{C6}$. The network contains 124 directed supply-demand edges. All risk factors and enterprise-node states are binary variables$\{T, F\}$, where T denotes risk occurrence or node disruption, and F denotes no risk occurrence or normal node operation. Given the occurrence probability P_{ij} and impact intensity u_{ij} of risk factor i at node j, the node's own disruption probability is aggregated in Noisy-OR form:

$$P\left(V_j^{Risk} = T\right) = 1 - \prod_{i \in \Psi_j} \left(1 - u_{ij}\right)$$

where Ψ_j is the set of risk factors triggered in a given draw.

Ripple effects propagate down the directed network through conditional-probability parameters w_{rj} calibrated from trade-flow shares:

$$P\left(V_j^{pro} = T\right) = min\left(1, \sum_r P(O_r = T) \cdot w_{rj}\right)$$

The integrated disruption probability of node $P(V_j = T)$ is the maximum of the two channels, max $\left\{P\left(V_j^{Risk} = T\right), P\left(V_j^{pro} = T\right)\right\}$. This continuous probability is passed downstream layer by layer. The terminal disruption risk exposure (DRE) of China's refined cobalt supply is defined as:

$$DRE = (disrupted\ Chinese\ refined\ cobalt\ supply) \\ /\ (total\ Chinese\ refined\ cobalt\ supply) \in [0,1]$$

The probability distribution of DRE is obtained through 100 000 Monte Carlo draws under three states: an optimistic state in which risk-factor probabilities equal 0.6 times their most-likely values, a most-likely state, and a pessimistic state in which risk-factor probabilities equal 1.2 times their most-likely values. For each draw under state S, DRE is calculated as the weighted sum of disruption probabilities across the five refiners, with weights w_i defined by inflow shares:

$$DRE_S = \sum_{ref=1}^{5} P\left(O_{ref} = T\right) \cdot w_{ref}$$

The full probability distribution of DRE_S is then embedded in the cobalt supply module of DRCCGE. Because refined cobalt production is constrained by the supply of cobalt ore as a fixed factor, a conventional supply function may fail to capture the resource constraint adequately. This study uses a Logistic function to represent the price response of resource supply:

$$ffcs_{cob} = \frac{fcMax_{cob}}{1 + \alpha ff_{cob} e^{-\gamma ff_{cob} \frac{pff_{cob}}{pindex}}} \cdot (1 - DRE)$$

The cobalt-ore factor supply has an exogenous theoretical maximum, $fcMax_{cob}$,which represents the mining limit of cobalt ore over the simulation period. When the real factor price, $pff_{cob}/pindex$, is low, supply $ffcs_{cob}$ is also low. As the real price rises, supply increases and approaches $fcMax_{cob}$ asymptotically, but never reaches that ceiling. The parameters $fcMax_{cob}$、αff_{cob}, and γff_{cob} determine the location and curvature of the cobalt-ore supply function. Multiplication by (1-DRE) converts the probabilistic disruption measure into an effective contraction in available cobalt-ore supply, thereby linking the BN-MC supply-chain risk module to the macroeconomic model.

3 Data

The data foundation has two components: a social accounting matrix that represents the base-year economic structure, and model parameters that govern the response of economic agents. The construction and calibration strategy are as follows.

(1) Construction of the social accounting matrix and sector disaggregation

The study combines the 2023 national input-output table, government revenue and expenditure data, household income and expenditure data, employment statistics, and related official sources to build a 42-sector social accounting matrix (SAM). The data sources include the 2023 input-output table released by the National Bureau of Statistics, China Statistical Yearbook 2024, China Economic Census Yearbook 2023, China Labour Statistical Yearbook 2024, China Taxation Yearbook 2024, and the 2023 national fiscal final accounts report.

Refined cobalt is produced by smelting and processing cobalt ore. To represent the transmission mechanism of the cobalt industrial chain more precisely, the refined cobalt sector is separated from the broader "non-ferrous metal smelting and rolling processing" sector. The separation follows a simple principle: preserve the accuracy of aggregate totals while using economically defensible disaggregation ratios.

Total output and total input of refined cobalt are determined first. Domestic gross output is calculated from the production volumes and prices of electrolytic cobalt, tricobalt tetroxide, and cobalt sulphate. Production data are taken from Baiinfo, and price data are taken from the London Metal Exchange (LME). Under the accounting logic of the SAM, total input equals total output, which then fixes the sector's total input.

The input structure of the refined cobalt sector is identified from the financial reports of major cobalt refiners. The principal domestic refined cobalt producers include Huayou Cobalt, Hanrui Cobalt, and Tengyuan Cobalt, which together account for more than 80% of China's output. Their 2023 annual reports indicate approximate input shares of 85.75% for raw materials, 4.52% for auxiliary materials, 1.56% for labour, 2.52% for energy, 0.25% for transport and miscellaneous charges, and 5.42% for other inputs. The allocation of these items to more detailed SAM sectors is further split according to the input structure of the "non-ferrous metal smelting and rolling processing" industry.

The output-use structure of refined cobalt is determined from material-flow analysis. Material-flow analysis is one of the most effective methods for tracing the pathway of materials from production to use, including mining and beneficiation, smelting, product processing, manufacturing, use, and waste management. Existing studies have already mapped China's cobalt material flows. This study collects and harmonises published cobalt material-flow evidence to determine the share of China's refined cobalt used as intermediate use, assuming that the domestic and imported product shares are identical. Refined cobalt use corresponds to the product-processing and manufacturing stage. The sectoral allocation is then assigned according to flow destinations, including consumer-electronics batteries, NEV batteries, energy-storage batteries, superalloys, hard alloys, magnetic alloys, glass and ceramics, and catalysts, with each category mapped to its corresponding SAM sector. Because refined cobalt is used mainly as an intermediate input into other products and has no final household consumption, changes in refined cobalt inventories are taken from LME data.

Production and use also involve imports and exports. Trade data are drawn from UN Comtrade and are incorporated into the refined cobalt account so that domestic production, intermediate use, inventory change, and external trade remain mutually consistent within the SAM.

(2) Parameter calibration

The CGE model parameters include share parameters and elasticity parameters. Share parameters are calibrated directly from the SAM, ensuring that the base-year equilibrium replicates the observed accounting structure. Elasticity parameters are assigned exogenously with reference to the relevant CGE and energy-economy modelling literature. The main elasticity settings are reported in the Appendix.

4 Scenario Design

The scenario design is structured to identify the channels through which cobalt supply-chain disruption affects macroeconomic performance and the energy structure under China's NDC target. The baseline scenario first describes China's long-run socioeconomic development and the continuation of existing mitigation policies. The NDC target scenario then strengthens the carbon constraint using China's third-round NDC announced in 2025, thereby representing the energy-economic transformation under deep decarbonisation. Finally, the cobalt supply-risk scenarios add disruptions of varying severity on top of the NDC scenario to identify how critical-mineral risk perturbs the carbon-neutral transition pathway. By layering exogenous shocks in this order, the simulations separate the marginal effects of mitigation policy from the marginal effects of cobalt supply shocks.

(1) Baseline scenario

The baseline scenario combines projections from authoritative domestic and international institutions with research on China's "15th Five-Year Plan". It uses core socioeconomic parameters, including population and labour force, economic growth, urbanisation, the investment-consumption structure, and total factor productivity, to describe the objective trend of China's long-run development. This provides a common reference path for comparing the NDC target and cobalt supply-risk scenarios.

Future population and labour-force growth are based on the United Nations World Population Prospects medium-fertility scenario and joint projections from the China Population and Development Research Center. China's population entered negative growth in 2022 and is expected to decline by about 4 million people per year over the following decade. The total population is set at 1.42 billion in 2030, 1.38 billion in 2035, and 1.29 billion in 2060. The share of the working-age population (15-64 years) falls by 0.4 percentage points per year on average, leaving working-age populations of 920 million in 2027 and 870 million in 2035. Average years of schooling among the working-age population rise from 11.21 years in 2024 to 12.4 years in 2035, so gains in human-capital quality partly offset the decline in demographic quantity.

China's long-run economic growth path is set after reviewing projections from the Development Research Center of the State Council, the World Bank (WB, 2024), the International Monetary Fund (IMF, 2024), and the International Energy Agency (IEA, 2024). The assumed average annual real GDP growth rates are 5.2% for 2021-2025, 4.5% for 2026-2030, 3.8% for 2031-2035, 3.2% for 2036-2040, 2.8% for 2041-2050, and 2.5% for 2051-2060. These assumptions imply real GDP of RMB180 trillion in 2030 at constant 2020 prices, with per capita GDP exceeding US$18,000. By 2035, GDP reaches RMB217 trillion, per capita GDP reaches US$22,000, and China crosses the high-income threshold on a sustained basis. By 2060, GDP reaches RMB410 trillion and per capita GDP is about US$32,000.

China has entered the later stage of urbanisation, with growth in the urbanisation rate gradually slowing. The scenario assumes that the urbanisation rate increases by 0.68 percentage points per year on average from 2025 to 2035, reaching 68.5% in 2027 and 75% in 2035. The registered urbanisation rate rises to 70% over the same period, implying that the citizenship transition of the migrant agricultural population is largely completed. Population continues to concentrate in urban agglomerations, and the eastern region maintains more than 40% of the permanent-resident population. Drawing on international experience and China's ageing trend, the investment rate is assumed to decline by 1.06 percentage points per year on average from 2025 to 2035, reaching 40.6% in 2027 and about 30% in 2035. The saving rate declines in parallel, and the final-consumption rate reaches 60% in 2035, marking the consolidation of a domestic-demand-led growth pattern. Investment shifts towards high-technology manufacturing, green energy, and the digital economy, while the share of investment in energy-intensive industries continues to contract. Taking account of the remaining scope for technological catch-up and indigenous innovation capacity, total factor productivity growth in the baseline is set at around 1.5% per year.

The carbon-mitigation constraint in the baseline follows the level of ambition in China's first-round NDC submitted in 2015. CO_2 emissions peak around 2030 and decline only slowly thereafter, remaining at roughly 7 billion tonnes in 2060. Carbon intensity per unit of GDP falls by 60%-65% from the 2005 level by 2030, and non-fossil energy reaches about 20% of primary energy consumption.

The model adopts a neoclassical factor-market closure. Capital and labour move freely across sectors, and factor prices are determined by supply-demand equilibrium. Capital accumulation follows the perpetual-inventory method with a 5% depreciation rate. The labour market is assumed to clear at full employment with flexible wages. The balance of payments is approximately balanced, and the real exchange rate is determined endogenously.

(2) NDC target scenario

The NDC target scenario retains the socioeconomic assumptions of the baseline but introduces stronger mitigation policy through the carbon-emissions constraint. The mitigation stringency is based on the third-round Nationally Determined Contribution (NDC) announced by China at the United Nations climate summit in 2025. Economy-wide CO_2 emissions peak early in 2028 at 12.56 billion tonnes. By 2035, economy-wide net greenhouse gas emissions fall by 7%-10% relative to the peak, and by 2060 they fall further to 940 million tonnes. Residual emissions are balanced by CCS and ecological carbon sinks to achieve near-zero net emissions. This pathway is imposed as an exogenous emissions-cap constraint. The primary energy mix becomes cleaner more rapidly, the power system undergoes deep decarbonisation, and new-energy vehicle penetration accelerates. EV penetration reaches 53.9% in 2025, 72.0% in 2030, 92.0% in 2040, 98.0% in 2050, and 99.0% in 2060. Road transport is therefore almost fully electrified, with only a very small residual share reserved for difficult-to-electrify uses such as aviation, ocean shipping, and heavy freight. The national carbon market covers the main high-emitting industries.

(3) Cobalt supply-chain disruption scenarios under the NDC target

The cobalt disruption scenarios inherit the NDC target settings and introduce an exogenous cobalt supply-chain shock to identify how critical-mineral risk perturbs the carbon-neutrality pathway. Because cobalt supply-chain risk is multi-sourced and highly uncertain, the shock is quantified with the BN-MC framework developed above. China's cobalt supply chain is represented as a directed acyclic graph with 76 main nodes and 119 directed edges: 34 global mines, 37 primary refiners, and 5 core Chinese refiners. The framework identifies 12 core risk factors. Upstream mine nodes are exposed to six risk categories: geopolitical conflict, climate disaster, geological risk, environmental compliance, infrastructure failure, and labour conflict. Refining-enterprise nodes are exposed to six risk categories: geopolitical conflict, trade sanctions, ESG compliance, armed conflict, logistics disruption, and climate disaster. The prior probabilities of all triggered risks are calibrated from multiple authoritative data sources, including the World Bank Worldwide Governance Indicators, the EM-DAT international disaster database, and the global geopolitical risk index. After 100 000 Monte Carlo simulations, the cumulative probability distribution of China's expected disruption risk exposure at the refined cobalt supply end is obtained, as shown in Figure 2.

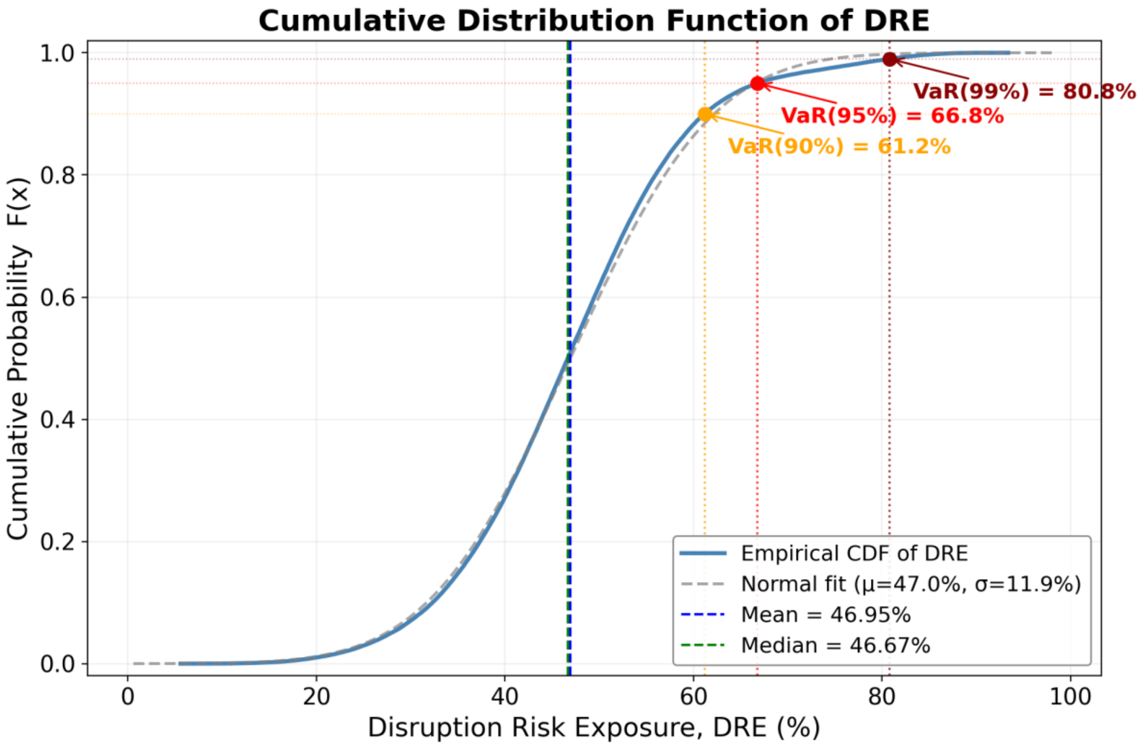

Figure 2. Cumulative probability distribution of supply disruption risk exposure at China's refined cobalt

Based on this risk measurement, the study considers a cobalt supply-chain disruption occurring in 2027. This timing is analytically important because it falls in China's critical carbon-peaking period and during the accelerated expansion of the new-energy industry, when cobalt supply-chain vulnerability is especially salient. Instead of using a conventional design with a few discrete shock points, the simulations impose a continuous range of shocks, DRE∈(0%,80%], on top of the NDC reference scenario. The upper bound of 80% corresponds to the 99th-percentile extreme tail risk in the BN-MC simulations. This design reduces the subjective bias of selecting arbitrary discrete disruptions, covers the full risk spectrum from routine mild disturbance to extreme events, and captures the response profiles of macroeconomic output and the energy structure with greater precision. It also permits the model results for different shock intervals to be weighted by the probability-density distribution produced by the BN-MC model, yielding expected risk losses that account for both event probability and damage severity.

5 Results

5.1 GDP impacts of cobalt supply-chain disruption

GDP losses under the cobalt supply-chain disruption scenarios, relative to the baseline, have two components. The first is the long-run transition cost generated by mitigation policy under the NDC target. The second is the additional short-run loss triggered by cobalt supply-chain disruption. These losses differ markedly in intensity, duration, and mechanism.

Under the NDC scenario, GDP follows a clear three-stage trajectory: short-run gains, expanding medium-run losses, and a modest narrowing of losses in the long run. During 2027-2030, GDP in the NDC scenario is substantially higher than in the baseline. A decomposition of sectoral output and demand shows that this short-run gain is driven by the deep electrification pathway that the NDC commitment forces from 2027 onward. The pathway stimulates demand and output in clean-energy and electrification-related sectors. Solar power output is 12.5%-41.7% higher than in the baseline, and NEV output is 4.9%-11.5% higher. Coal power output, by contrast, is only 7.3%-18.6% lower than in the baseline. The expansion of higher-value-added clean-energy sectors therefore more than offsets the contraction of high-carbon sectors at the aggregate level, generating a positive short-run GDP deviation.

After 2031, the carbon constraint tightens further. Rising carbon prices suppress energy-intensive industrial output and transmit to downstream consumption, services, and export competitiveness through intermediate use prices and final electricity prices. At this stage, the negative effect of policy exceeds the dividend from clean-sector expansion, and GDP losses increase continuously. The GDP loss rate reaches -0.31% in 2040 and widens to -0.49% in 2050. After 2050, policy costs narrow slightly, and the GDP loss rate falls back to -0.46% by 2060, an improvement of about 0.032 percentage points relative to 2050. This late-stage easing is mainly driven by the cumulative effect of long-run capital accumulation. Under the NDC scenario, society must continue to invest in fixed assets to support deep electrification and the scaled operation of carbon capture, utilisation, and storage (CCS). By 2050, total fixed-asset investment shifts from a long-run negative deviation to +0.158%, while the baseline has already entered the natural decline phase of the investment rate. The capital-stock gap between the two scenarios is gradually filled in later periods, helping GDP losses to contract.

Compared with the gradual transition cost caused by NDC policy itself, the additional short-run losses from cobalt supply-chain disruption are much larger. In 2027, when disruption exposure is at the expected BN-MC level of approximately DRE=47%, GDP falls by 0.15% relative to the baseline. The marginal contribution of the cobalt shock is about 0.144 percentage points, or roughly US$31.3 billion, accounting for about 96% of the total loss. Under the extreme disruption scenario of DRE=80%, GDP falls by 0.29% relative to the baseline. The cobalt shock contributes 0.283 percentage points, or approximately US$61.4 billion, accounting for about 98% of the total loss.

The marginal GDP loss caused by a unit change in cobalt supply is highly heterogeneous. When DRE deteriorates from 10% to 20%, the incremental GDP loss is 0.028 percentage points. When DRE deteriorates from 70% to 80%, the incremental loss expands to 0.048 percentage points. The marginal loss per unit of disruption intensity therefore rises by about 70%. This result implies that an equal investment in strategic reserves or procurement diversification yields a higher avoided-loss return in high-DRE intervals. Reducing DRE from 80% to 70% avoids about 1.7 times the GDP loss avoided by reducing DRE from 20% to 10%. Risk-mitigation policy should therefore prioritise preventing DRE from entering the severe-disruption range.

In the long run, the binding emissions cap causes capital released from shrinking EV and battery sectors to be reallocated across non-fossil energy technologies, including wind, solar, nuclear, CCS, and non-electric alternatives for road transport. This process builds a stock of clean-energy capital. The passively accelerated deployment of clean energy begins to take effect after 2040 and substantially eases mitigation pressure on non-electric technologies and non-transport sectors. As a result, the GDP deviation of cobalt disruption scenarios relative to the NDC scenario turns from negative to positive around 2040. In other words, the cobalt shock does not continue to drag on GDP in the long run; under the binding NDC constraint, it instead produces GDP that is slightly higher than in the no-disruption NDC scenario. Sections 5.2 and 5.3 provide direct evidence for this long-run reversal from the perspectives of carbon emissions and the energy structure.

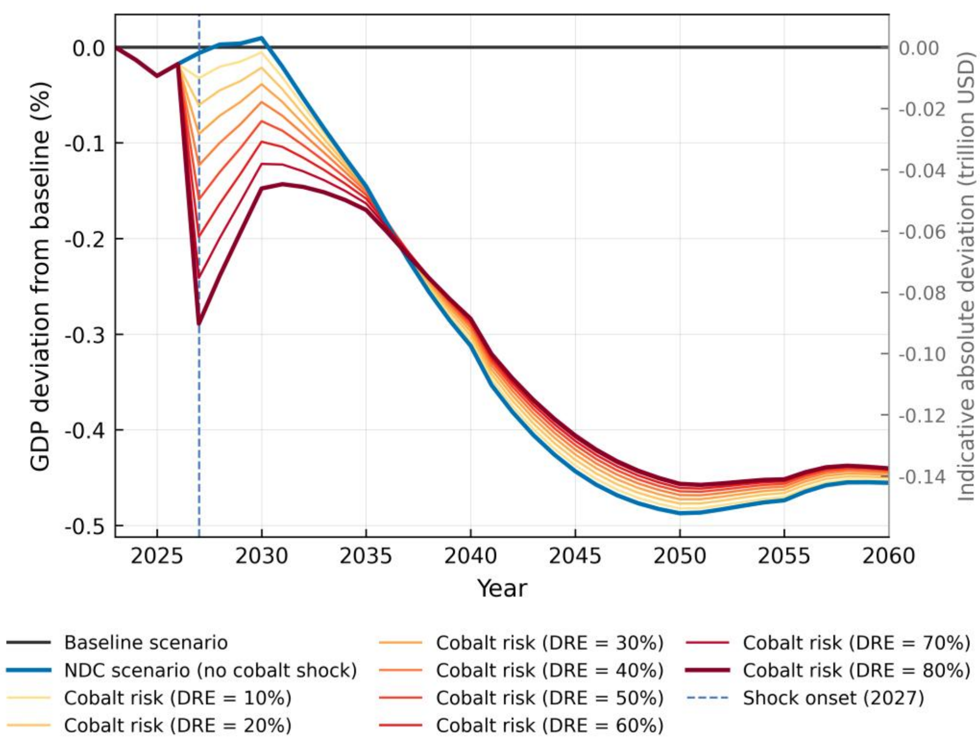

Figure 3. Impacts of cobalt supply-chain disruption on China's GDP

Note: The vertical axis reports the percentage deviation of GDP from the baseline scenario. Curves include the NDC scenario and cobalt supply-chain disruption scenarios with DRE=10%-80% (NDC-DRE10-80). The dashed vertical line in 2027 marks the shock year.

The scale mismatch is striking. China's refined cobalt sector has a base-year output of about US$3.46 billion in 2027, only 0.016% of real GDP in that year. Yet when 80% of refined cobalt supply is disrupted, the economy-wide GDP loss reaches US$61.4 billion, or 0.283% of total GDP. China's high external dependence on cobalt resources means that the price shock triggered by cobalt disruption cascades downstream along the refined cobalt-traction battery-NEV chain. Combined with cross-sectoral reallocation of capital and labour, this upstream resource bottleneck generates a macroeconomic loss far larger than the sector's direct footprint.

Figure 4 uses the BN-MC framework to characterise the cumulative distribution of GDP impacts caused by cobalt supply-chain disruption from 2027 to 2060. For any given year t, taking the cross-section along the vertical axis gives the probability distribution that the GDP loss or gain in year t does not exceed a given magnitude x. This representation reveals the risk structure of the cobalt supply chain. Relative to the NDC scenario, the expected GDP loss caused by cobalt supply-chain disruption in 2027 is US$31.3 billion, and the 99th-percentile tail value at risk (VaR_{99}) is US$62.2 billion. Over time, the probability distribution of GDP impacts shifts systematically from loss-dominated to gain-dominated outcomes relative to the NDC scenario.

The reversal from losses to gains is concentrated between 2035 and 2040. In 2035, the 99th-percentile value of the GDP-impact distribution remains in the loss range, with an extreme loss of about US$7.06 billion. From 2040 onward, this percentile moves into the gain range, with a maximum gain of about US$330 million. At the same time, uncertainty around GDP impacts narrows substantially. The coefficient of variation, defined as the ratio of the standard deviation to the mean, falls from 30.7% in 2027 to 20.6% in 2050. The long-run reversal from GDP losses to gains is therefore not only robust in expectation; its probability also becomes more certain.

Overall, the probability-distribution results from the BN-MC framework show that the long-run GDP-impact distribution shifts systematically from a loss range to a gain range and that impact uncertainty converges markedly. This provides a quantitative basis for more targeted long-term policies to manage supply-chain risk.

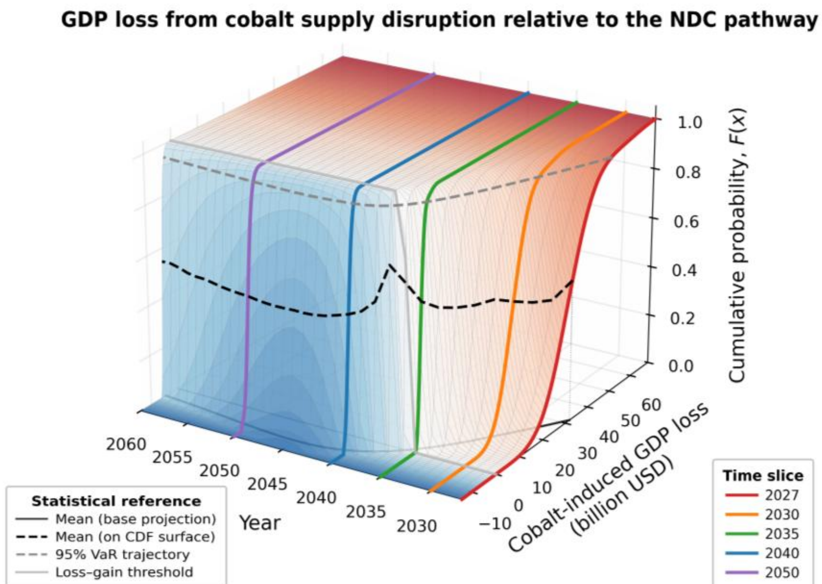

Figure 4. Cumulative probability distribution of GDP losses induced by cobalt supply-chain disruption

Note: The cumulative distribution function of GDP losses is obtained by mapping the DRE cumulative distribution from 100 000 BN-MC Monte Carlo simulations. The figure marks the mean trajectory and the 99th-percentile tail value at risk.

5.2 CO_2-emissions impacts of cobalt supply-chain disruption

Figure 5a shows that cobalt supply-chain disruption has only a limited effect on total CO_2 emissions. Emissions under the disruption scenarios remain close to those under the NDC scenario. Under the extreme DRE=80% shock, total CO_2 emissions in 2027 are 12 496.37 Mt, only 2.55 Mt higher than in the NDC reference scenario, an increase of 0.020%. This limited aggregate response is important to interpret correctly. The absence of a large increase in total CO_2 emissions is not caused by endogenous abatement mechanisms such as technology substitution or energy-efficiency improvement. It reflects an offset between passive emissions reductions caused by economic contraction and emissions increases in sectors such as transport.

At the sector level, Figure 5b shows that cobalt scarcity constrains EV deployment, sharply reduces EV penetration, and raises CO_2 emissions from the transport sector. Under DRE=80%, EV penetration in 2027 is 8.18% lower than in the NDC scenario, and transport-sector CO_2 emissions are 141.09 Mt higher. This large increase in transport emissions does not translate into a comparable increase in economy-wide CO_2 emissions because passive abatement from economic contraction offsets much of it. Figure 5c shows that cobalt supply-chain disruption propagates through the industrial chain and suppresses output in downstream electricity-intensive manufacturing sectors, including batteries, machinery manufacturing, and metal smelting. Lower electricity demand then reduces output from the high-carbon coal power sector. Under DRE=80%, coal power emissions fall by 98.45 Mt in 2027, offsetting more than 70% of the increase in transport emissions.

These results show why climate-policy assessment cannot rely only on aggregate emissions indicators. Total CO_2 emissions can appear stable even when the structure of decarbonisation deteriorates sharply. In this case, the apparent stability of emissions hides a setback in transport electrification and a passive contraction of industrial activity, both of which are central to the real economic and technological consequences of critical-mineral supply risk.

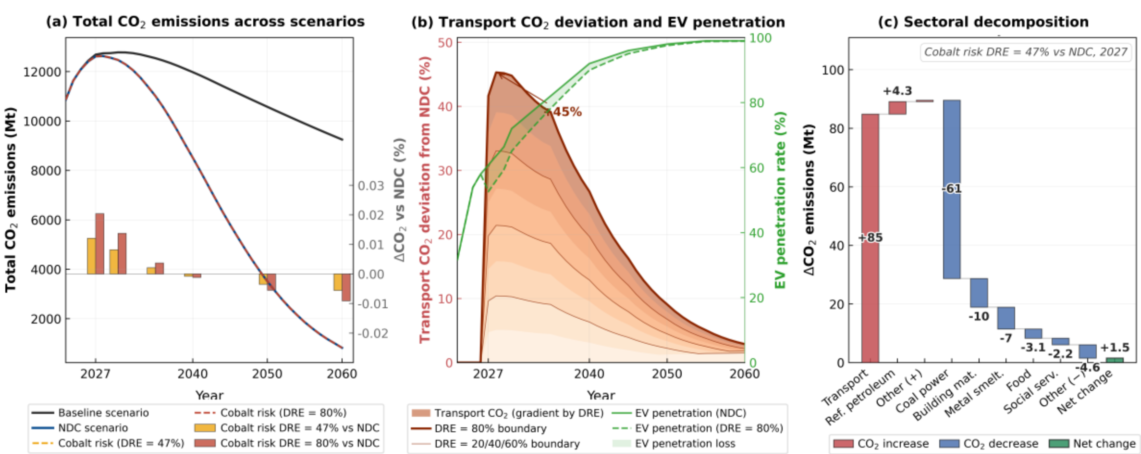

Figure 5. Impacts of cobalt supply-chain disruption on CO_2 emissions

Note: (a) China's total CO_2 emissions trajectories from 2023 to 2060 under the baseline, NDC, NDC+DRE=47%, and NDC+DRE=80% scenarios; (b) percentage deviation of transport-sector CO_2 emissions from the NDC scenario during 2023-2060 (left axis) and EV penetration (right axis); (c) sectoral CO_2 changes in 2027 under the DRE=47% scenario.

5.3 Energy-structure impacts of cobalt supply-chain disruption

Figure 6a shows the evolution of China's primary energy structure under the NDC scenario. Total energy consumption grows moderately, while fossil energy exits the system more rapidly. In 2025, China's total primary energy consumption is 5494 Mtce. Coal, oil, and natural gas account for 18.5%, 36.5%, and 6.5%, respectively, and non-fossil energy accounts for 38.5%. By 2060, total energy consumption rises to 10396 Mtce as the economy grows and electrification deepens. The fossil-energy share falls sharply: coal, oil, and natural gas decline to 3.5%, 5.1%, and 1.8%, respectively, while the non-fossil energy share rises to 89.7%. The power sector undergoes an even more pronounced structural adjustment (Figure 6b). Total electricity generation is 9.06 PWh in 2025, with coal power accounting for 65.7% and remaining the dominant source of generation. Solar, wind, and nuclear power account for 5.2%, 7.8%, and 4.0%, respectively. As wind and solar capacity continue to expand and coal power is phased down in an orderly way, total electricity generation reaches 28.64 PWh in 2060. The coal power share falls to 1.2%, while solar and wind together account for 80.6%, producing a deeply decarbonised power system dominated by non-fossil energy.

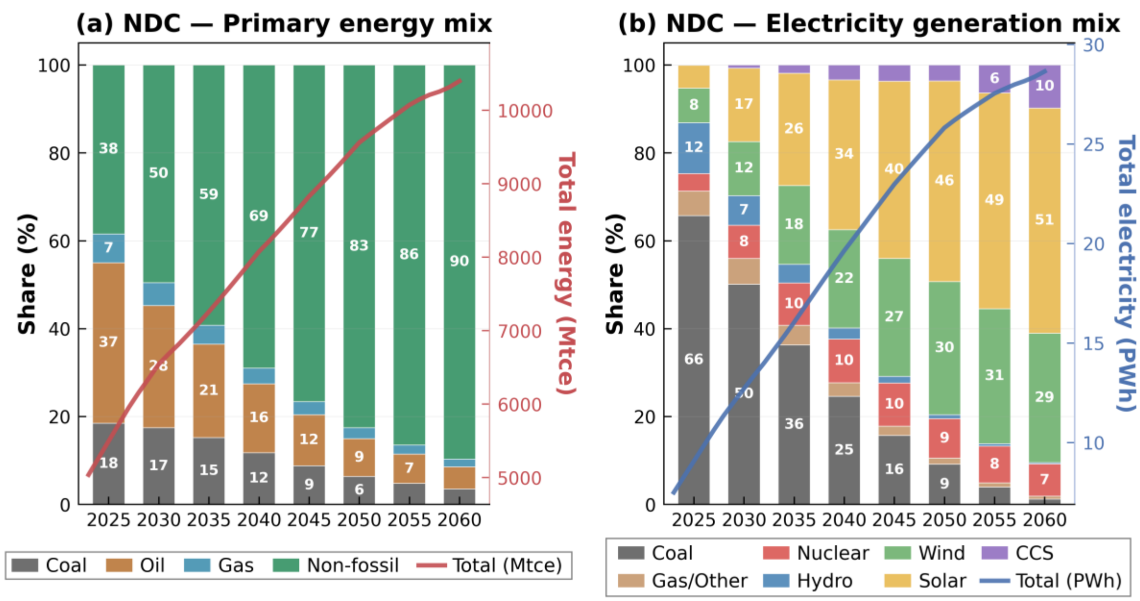

Figure 6. Evolution of China's energy structure under the NDC scenario

Note: (a) Primary energy consumption structure (left axis: shares of coal, oil, natural gas, and non-fossil energy, %; right axis: total primary energy consumption, Mtce); (b) electricity generation structure (left axis: shares of coal power, gas and others, nuclear, hydropower, wind, solar, and CCS, %; right axis: total generation, PWh).

Figure 7 describes the evolution of primary energy consumption under cobalt disruption. In the initial shock period, the fossil-energy share rises. Under DRE=80%, total primary energy consumption in 2027 increases by a net 47 Mtce relative to the NDC reference scenario. Oil consumption increases by 55 Mtce, coal consumption increases by 4 Mtce, and non-fossil energy consumption falls by 12 Mtce. Around 2035, the change in non-fossil energy consumption reverses. Under DRE=80%, non-fossil energy consumption is 1 Mtce higher in 2035, 6 Mtce higher in 2040, and 10 Mtce higher in

2050. Over the same period, the increase in oil consumption falls from 55 Mtce in 2027 to 1 Mtce in 2060, and the initial rise in the fossil-energy share gradually converges. At the BN-MC expected level of DRE=47%, non-fossil energy consumption is 6 Mtce higher in 2050 and remains 5 Mtce higher in 2060, following the same direction as the extreme scenario. The transmission mechanism is that, under the tight NDC policy constraint, capital released from downstream cobalt-using sectors such as NEVs and traction batteries cannot return fully to the original chain. Through the equilibrium mechanism, it is reallocated to non-fossil energy technologies such as wind, solar, nuclear, and CCS, generating a long-run net increase in non-fossil energy consumption.

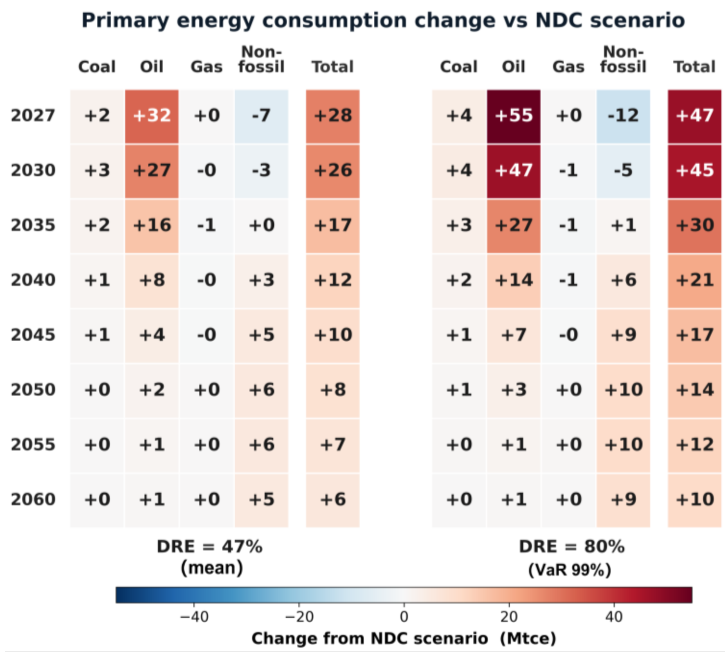

Figure 7. Impacts of cobalt supply-chain disruption on the primary energy consumption structure

Note: Changes in energy consumption relative to the NDC scenario. The left panel reports the DRE=47% scenario (BN-MC mean), and the right panel reports the DRE=80% scenario (extreme tail risk). The vertical axis is year, and the horizontal axis shows coal, oil, natural gas, and non-fossil energy. The colour scale represents changes in energy consumption: red indicates higher consumption, and blue indicates lower consumption.

Figure 8 further decomposes the electricity generation structure. In the initial shock period, cobalt supply-chain disruption suppresses downstream electricity-intensive manufacturing output and reduces total electricity demand, causing generation from all technologies to fall simultaneously. Under DRE=80%, net electricity generation in 2027 is 68 TWh lower than in the NDC reference scenario. Coal power generation falls by 54 TWh, accounting for 79% of the total reduction. Solar, wind, nuclear, and hydropower generation decline by 2.6 TWh, 4.8 TWh, 3.8 TWh, and 3.5 TWh, respectively. In 2035, under DRE=80%, coal power generation remains 14 TWh lower, but solar, wind, and nuclear generation all turn positive, increasing by 4.4 TWh, 3.9 TWh, and 2.4 TWh, respectively. The reduction in net generation narrows to 3 TWh. In 2040, net generation turns positive for the first time, rising by 18 TWh. Solar and wind generation increase by 11.7 TWh and 10.1 TWh, respectively, while the coal power reduction shrinks to 9 TWh. In 2050, the positive increase in net generation expands further to 35 TWh. Solar and wind generation together increase by 33.9 TWh, and the reduction in coal power generation narrows to 3 TWh. By 2060, the positive increase in net generation remains at 31 TWh, and the coal power reduction approaches zero at only 0.13 TWh. At the BN-MC expected level, the evolution of the generation structure is consistent with the extreme scenario: in 2050, net generation is 20 TWh higher, about 58% of the increase in the extreme scenario.

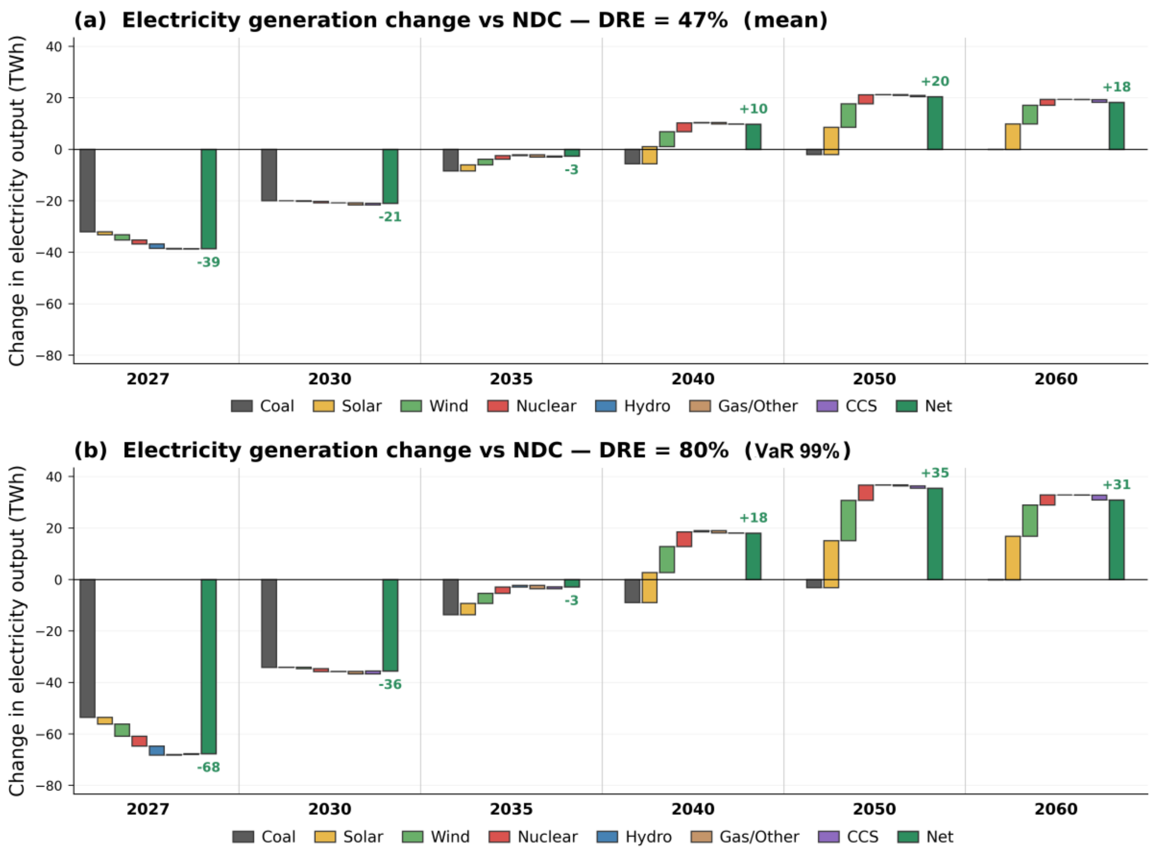

Figure 8. Impacts of cobalt supply-chain disruption on the electricity generation structure

Note: (a) DRE=47% (BN-MC mean); (b) DRE=80% (extreme tail risk). Each group displays net changes in the order coal power → solar → wind → nuclear → hydropower → gas and others → CCS. Thin grey lines connect the cumulative height of adjacent bars to form a waterfall chart, and the zero line is shown as a thick solid line.

6 Conclusions and policy implications

As China's NDC target accelerates and DRC cobalt export controls continue to evolve, the channels and magnitude through which cobalt supply-chain disruption may affect China's energy transition have become a critical question for both decarbonisation and industrial supply-chain security. This study couples a BN-MC model with the DRCCGE model and introduces uncertainty in cobalt supply disruption into a macroeconomic equilibrium framework. It systematically characterises how cobalt disruptions of different intensities affect China's GDP, CO_2 emissions, and energy structure over the long run. Three main conclusions follow.

Firstly, cobalt-related sectors are tiny in direct economic scale, but they exert a strong leverage effect on the macroeconomy, and their GDP impacts adjust dynamically over time. Cobalt mining, beneficiation, and refining account directly for less than 0.01% of China's GDP, yet industrial-chain linkages allow shocks in these sectors to generate macroeconomic impacts far larger than their own scale. Under the extreme DRE=80% disruption scenario, China's real GDP in 2027 falls by 0.29% relative to the baseline. The marginal contribution of the cobalt shock is about US$61.4 billion, and its 99th-percentile tail value at risk is about US$62.2 billion. In the long run, around 2040, the GDP deviation under the cobalt disruption scenario relative to the NDC scenario turns from negative to positive. This reversal reflects endogenous factor reallocation within the economic system. The marginal GDP loss per unit of disruption intensity also rises with DRE, meaning that avoided-loss efficiency is higher in high-DRE ranges. Risk-mitigation policy should therefore focus first on preventing DRE from entering severe-disruption intervals.

Secondly, the emissions effect of cobalt disruption is asymmetric: the aggregate impact is small, but the structural imbalance is substantial. The weak aggregate change is not caused by endogenous abatement; it is the passive result of economic contraction. Under the extreme DRE=80% scenario, transport-sector CO_2 emissions in 2027 are 141.09 Mt higher than in the NDC scenario. The contraction of downstream electricity-intensive manufacturing and coal power creates an offsetting reduction, so economy-wide CO_2 emissions rise by only 2.55 Mt, or about 0.020%. This small aggregate movement is essentially passive abatement caused by GDP loss. Assessments of critical-mineral supply risk should therefore not rely only on total CO_2 emissions indicators. They must examine sectoral pathways to avoid allowing aggregate data to conceal structural risk.

Thirdly, cobalt disruption reshapes the energy and power structures over the long run and accelerates parts of the energy transition. Under the NDC policy constraint, cobalt supply disruption pushes capital away from EVs and batteries and towards non-fossil energy fields, including wind, solar, nuclear, and CCS. This reallocation improves the primary energy and electricity structures. In 2050, non-fossil energy consumption under the cobalt disruption scenario is 10 Mtce higher than in the NDC scenario, while fossil-energy consumption, including coal and oil, contracts. The non-fossil energy share rises. Net electricity generation is 35 TWh higher than in the NDC scenario, wind, solar, and nuclear output grow faster, and the thermal-power share falls further. These results reveal a long-run interaction between critical-mineral supply risk and carbon-constrained policy: disruption is costly in the short run, but the binding emissions cap redirects adjustment towards other low-carbon technologies.

Several policy implications follow from these findings.

Firstly, design the strategic reserve for critical minerals to match the short-run distribution of disruption probabilities, and rely on trade diversification to lower long-run exposure. On the reserve side, minerals with a small value share but high physical importance should enter the strategic reserve list. Reserve volumes can be calibrated to the economic losses estimated under extreme-disruption scenarios, with a dynamic rotation mechanism to contain holding costs. A central-reserve-dominant, enterprise-reserve-supplementary structure avoids the duplication that arises from fragmented sub-national stockpiles. On the trade side, leading firms should be encouraged to undertake upstream equity investment and long-term offtake agreements in non-DRC producers such as Indonesia, the Philippines, and Australia, supported by bilateral and multilateral mineral cooperation with major resource countries. Fiscal, financial, and diplomatic instruments can share the political risk of overseas investment, but concentration of such instruments on a single destination must be avoided to prevent a new form of supply concentration.

Secondly, treat low- and cobalt-free chemistries and end-of-life battery recycling as two structural channels for reducing supply risk, recognizing the marginal substitution between them. On the substitution side, stable policy expectations for R&D and demonstration of LFP, manganese-rich cathodes, and sodium-ion batteries can guide automakers and battery firms toward cathode-chemistry diversification. Fiscal support tied to the external supply-risk level—stronger R&D incentives when risk rises—delivers a state-contingent, dynamic incentive rather than a static subsidy. On the recycling side, the extended producer responsibility (EPR) regime should be developed alongside traceability across mining, refining, manufacturing, and end-of-life recovery, so that retired batteries serve as a secondary supply channel for critical minerals. Because the two channels are marginal substitutes in reducing supply risk, the policy mix should be reweighted dynamically with external supply conditions and technology learning curves, avoiding double subsidization of the same marginal effect.

Thirdly, integrate critical-mineral supply risk into the climate policy assessment framework to prevent general-equilibrium offsets from masking sectoral consequences behind aggregate indicators. Our simulations show that disruption has a limited effect on economy-wide CO_2, yet markedly raises transport-sector emissions; the near-stability of the aggregate reflects passive contraction of electricity-intensive manufacturing and coal power generation rather than endogenous mitigation, and is achieved at a measurable welfare cost. Aggregate emission indicators alone therefore systematicall understate the sectoral consequences of mineral risk for NDC progress. Sector-level emission-sensitivity indicators should enter the medium- to long-term monitoring system, with differentiated metrics for transport, power, and electricity-intensive manufacturing. Mineral supply risk should also enter as an exogenous condition into the joint design of NEV subsidy phase-out, non-fossil power investment, and carbon-market allowance allocation, so that coordination losses from independently designed instruments can be reduced.

References

Acemoglu, D., Akcigit, U., & Kerr, W. (2016). Networks and the macroeconomy: An empirical exploration. NBER Macroeconomics Annual, 30(1), 273–335.

Armington, P. S. (1969). A theory of demand for products distinguished by place of production. IMF Staff Papers, 16(1), 159–178.

An, K., Zheng, X., Shen, J., et al. (2025). Repositioning coal power to accelerate net-zero transition of China's power system. Nature Communications, 16, 2311.

Boer, L., Pescatori, A., Stuermer, M., & Valckx, N. (2021). Energy transition metals. IMF Working Paper, WP/21/243.

Bressan, G., Roncoroni, A., Battiston, S., et al. (2025). Macroeconomic impacts of the Russia-Ukraine conflict transmitted through commodity supply chains: A CGE analysis. Communications Earth & Environment.

Burfisher, M. E. (2017). Introduction to Computable General Equilibrium Models (2nd ed.). Cambridge University Press.

Cerra, V., & Saxena, S. C. (2008). Growth dynamics: The myth of economic recovery. American Economic Review, 98(1), 439–457.

Cheng, A. L., Fuchs, E. R. H., Karplus, V. J., & Michalek, J. J. (2024). Electric vehicle battery chemistry affects supply chain disruption vulnerabilities. Nature Communications, 15, 2143.

Church, C., & Crawford, A. (2020). Minerals and the metals for the energy transition: Exploring the conflict implications for mineral-rich, fragile states. In M. Hafner & S. Tagliapietra (Eds.), The Geopolitics of the Global Energy Transition. Springer.

Cobalt Institute (2024). Cobalt Market Report 2024. Cobalt Institute, Brussels.

Ferris, M. C., & Munson, T. S. (1997). PATH 4.6: A complementarity solver. Mathematical Programming Series B, 76(1).

Garvey, M. D., Carnovale, S., & Yeniyurt, S. (2015). An analytical framework for supply network risk propagation: A Bayesian network approach. European Journal of Operational Research, 243(2), 618–630.

Graedel, T. E., Barr, R., Chandler, C., et al. (2012). Methodology of metal criticality determination. Environmental Science & Technology, 46(2), 1063–1070.

Greim, P., Solomon, A. A., & Breyer, C. (2020). Assessment of lithium criticality in the global energy transition and addressing policy gaps in transportation. Nature Communications, 11, 4570.

Guan, D., Wang, D., Hallegatte, S., et al. (2020). Global supply-chain effects of COVID-19 control measures. Nature Human Behaviour, 4, 577–587.

Gulley, A. L., Nassar, N. T., & Xun, S. (2018). China, the United States, and competition for resources that enable emerging technologies. Proceedings of the National Academy of Sciences, 115(16), 4111–4115.

Hubbert, M. K. (1956). Nuclear energy and the fossil fuels. Drilling and Production Practice, American Petroleum Institute.

IEA (2021). The Role of Critical Minerals in Clean Energy Transitions. International Energy Agency, Paris.

IEA (2024). World Energy Outlook 2024. International Energy Agency, Paris.

IEA (2025a). Critical Minerals Outlook 2025. International Energy Agency, Paris.

IEA (2025b). DRC ARECOMS Decision No. 004/2025: Cobalt Quota System. IEA Policies Database.

IPCC (2022). Climate Change 2022: Mitigation of Climate Change. Working Group III Contribution to the Sixth Assessment Report. Cambridge University Press.

Klimek, P., Obersteiner, M., & Thurner, S. (2015). Systemic trade-risk of critical resources. Science Advances, 1(10), e1500522.

Liang, Y., Kleijn, R., Newman, S. T., & van der Voet, E. (2022). Material requirements for low-carbon energy technologies: A quantitative review. Renewable and Sustainable Energy Reviews, 161, 112334.

Lofgren, H., Harris, R. L., & Robinson, S. (2002). A Standard Computable General Equilibrium (CGE) Model in GAMS. IFPRI Microcomputers in Policy Research, 5.

Manberger, A., & Johansson, B. (2019). The geopolitics of metals and metalloids used for the renewable energy transition. Energy Strategy Reviews, 26, 100394.

Olivetti, E. A., Ceder, G., Gaustad, G. G., & Fu, X. (2017). Lithium-ion battery supply chain considerations: Analysis of potential bottlenecks in critical metals. Joule, 1(2), 229–243.

Pearl, J. (1988). Probabilistic Reasoning in Intelligent Systems: Networks of Plausible Inference. Morgan Kaufmann.

Reuters (2025a). DRC suspends cobalt exports for four months as oversupply weighs on prices. Reuters News, 24 February 2025.

Reuters (2025b). Glencore halted some cobalt deliveries over Congo export ban. Reuters News, 11 June 2025.

Schrijvers, D., Hool, A., Blengini, G. A., et al. (2020). A review of methods and data to determine raw material criticality. Resources, Conservation and Recycling, 155, 104617.

Shao, L., Hu, X., Wang, Z., et al. (2024). Bayesian network–Monte Carlo assessment of cobalt supply chain disruption risks for China. Manuscript in preparation.

Shi, X., Heng, Y., Duan, M., et al. (2025). Critical mineral constraints pressure energy transition and trade toward the Paris Agreement climate goals. Nature Communications, 16, 4496.

Sovacool, B. K., Ali, S. H., Bazilian, M., et al. (2020). Sustainable minerals and metals for a low-carbon future. Science, 367(6473), 30–33.

Sun, X., Hao, H., Liu, Z., Zhao, F., & Song, J. (2019). Tracing global cobalt flow: 1995–2015. Resources, Conservation and Recycling, 149, 45–55.

Sun, X., Wang, P., Chen, W. Q., et al. (2024). Foreign direct investment as a buffer against critical-mineral supply risks. Nature Sustainability, 7, 672–681.

Sun, Y., Zhu, S., Wang, D., et al. (2024). Global supply chains amplify economic losses from extreme heat. Nature, 627, 797–804.

Tahvonen, O. (1997). Fossil fuels, stock externalities, and backstop technology. Canadian Journal of Economics, 30(4), 855–874.

Tang, B.-J., Guo, Y.-Y., Yu, B., & Harvey, L. D. D. (2021). Pathways for decarbonizing China's building sector under global warming thresholds. Applied Energy, 298, 117213.

UNCTAD (2024). Review of Maritime Transport 2024. United Nations Conference on Trade and Development, Geneva.

USGS (2024). Mineral Commodity Summaries 2024. U.S. Geological Survey, Reston, VA.

Verpoort, P. C., Gast, L., Hofmann, A., et al. (2024). The spatial pattern of renewable energy and supply-chain risks. Nature Energy, 9, 491–503.

Wang, P., Sun, Z., Hu, Y., et al. (2025). Total material requirements for the global low-carbon energy transition. Nature Communications, 16, 9203.

Wang, Y., Wang, J., Zhang, X., et al. (2025). A multi-sector CGE assessment of cobalt supply risks for China. Resources Policy.

Wei, Y. M., Zhang, X., Wang, J., et al. (2025). Critical mineral supply shocks under IPCC AR6 mitigation pathways: A global CGE assessment. Nature Communications.

Wing, I. S., Larsen, P. H., Carvallo, J. P., et al. (2025). A method to estimate the economy-wide consequences of widespread, long duration electric power interruptions. Nature Communications, 16, 3335.

Xu, C., Dai, Q., Gaines, L., Hu, M., Tukker, A., & Steubing, B. (2020). Future material demand for automotive lithium-based batteries. Communications Materials, 1, 99.

Yu, F., Wang, X., Liu, Y., et al. (2024). Reducing critical mineral demand from battery recycling: Pathways under different end-of-life scenarios. Resources, Conservation and Recycling, 200, 107308.

Zeng, A., Chen, W., Rasmussen, K. D., et al. (2022). Battery technology and recycling alone will not save the electric mobility transition from future cobalt shortages. Nature Communications, 13, 1341.

Zhao, Y., Liu, X., Wang, J., et al. (2025). Critical mineral supply shocks and energy transition in CGE frameworks: Evidence from China. Energy Economics.

Li, Shantong, & Zhai, Fan (1997). Yi ge Zhongguo jingji de ke jisuan yiban junheng moxing. Shuliang Jingji Jishu Jingji Yanjiu, 3, 38–44 (in Chinese).

Li, Shantong, & He, Jianwu (2009). Zhongguo ke jisuan yiban junheng moxing. Beijing: Jingji Kexue Chubanshe (in Chinese).

Li, S., He, J., & Liu, Y. (2010). A dynamic recursive CGE model for China: Theory and applications. Journal of Policy Modeling, 32(4), 432–447.

China Association of Automobile Manufacturers (2025). 2025 nian Zhongguo xinnengyuan qiche chanye fazhan lanpishu. Beijing: China Association of Automobile Manufacturers (in Chinese).